Fouling and performance of outer selective hollow fiber membrane in osmotic membrane bioreactor: Cross flow and air scouring effects

Van Huy Tran[a], Sungil Lim[a], Myoung Jun Park[a], Dong Suk Han[b], Sherub Phuntsho[a], Hyunwoong Park[c], Hideto Matsuyama[d], Ho Kyong Shon[a],*

[a] *Centre for Technology in Water and Wastewater (CTWW), School of Civil and Environmental Engineering, University of Technology Sydney (UTS), Australia*
[b] *Center for Advanced Materials, Qatar University, P.O. Box 2713, Doha, Qatar*
[c] *School of Energy Engineering, Kyungpook National University, Daegu 41566, Republic of Korea*
[d] *Research Center for Membrane and Film Technology, Department of Chemical Science and Engineering, Kobe University, 1-1 Rokkodai, Nada, Kobe 657-8501, Japan*

GRAPHICAL ABSTRACT
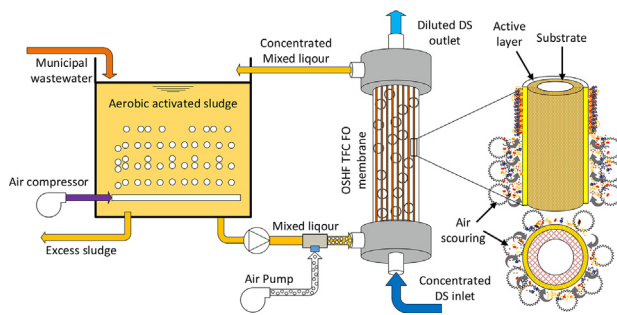
ARTICLE INFO

ABSTRACT

This study assessed impacts of cross-flow velocity (CFV) and air scouring on the performance and membrane fouling mitigation of a side-stream module containing outer-selective hollow fiber thin film composite forward osmosis membrane in osmosis membrane bioreactor (OMBR) system for urban wastewater treatment. CFV of draw solution was optimized, followed by the impact assessment of three CFVs on feed solution (FS) stream and periodic injection of air scouring into the side-stream module. Overall, the OMBR system exhibited high and stable performance with initial water flux of approximately 15 LMH, high removal efficiencies of bulk organic matter and nutrients. While FS's CFVs insignificantly affected the performance and membrane fouling, regular air scouring showed substantial impact with better performance and high efficiency in mitigating membrane fouling. These results indicated that periodic air scouring can be applied into the side-stream membrane module for efficient fouling mitigation without interruption the operation of the OMBR system.

1. Introduction

Osmotic membrane bioreactor (OMBR) is considered as emerging membrane technology for wastewater treatment and water reclamation. This OMBR system integrates forward osmosis (FO) process into a conventional membrane bioreactor (MBR) (Morrow et al., 2018a). Similar to FO process, OMBR is driven by the osmotic pressure difference between a highly saline draw solution (DS) and a low-salinity

---

* Corresponding author.
  E-mail address: hokyong.shon-1@uts.edu.au (H. Kyong Shon).

activated sludge feed solution (FS) separated by a semi-permeable FO membrane. Water permeate from the FS is drawn by the osmotic pressure to pass through the highly selective FO membrane to DS side. OMBR can be operated in re-concentration mode or dilution mode. In the first mode, OMBR operates as a water treatment system with the integration of a regeneration unit, which re-concentrates DS and produces purified water. The re-generation unit can be reverse osmosis (RO) process to form an OMBR - RO hybrid system as an alternative to the conventional MBR – RO system (Luo et al., 2017). OMBR helps to dilute draw solution using water reclaimed from wastewater, therefore, reducing the required energy for RO process and preventing pollutants and contaminants entering the draw solution loop. In osmotic dilution mode, when a water soluble fertilizer is used as a DS, OMBR can be used to dilute fertilizer by water drawn from activated sludge feed solution, the diluted fertilizer can then be used for direct or indirect irrigation (Kim et al., 2017).

The OMBR system is an attractive technology, being capable of producing high quality water product (Chang et al., 2019). The non-porous FO membrane, consisting of a highly selective layer, can provide the reliable and high rejection of pathogens, trace organic compounds, and ions contained in the activated sludge (Holloway et al., 2015b; Qiu and Ting, 2014b). OMBR system has the edge over conventional MBR system including higher quality water owing to its high selectivity of FO membrane compared to microfiltration or ultrafiltration used in MBR system (Achilli et al., 2009; Cornelissen et al., 2008). Recent OMBR studies also demonstrated the much higher removal efficacies of total organic carbon, ammonium, total nitrogen and phosphate than that achieved by MBR system (Holloway et al., 2015b; Qiu and Ting, 2014b). Moreover, due to the employment of osmotic pressure, OMBR system has lower fouling propensity with reversible fouling compared to irreversible fouling in conventional MBR or RO process using high hydraulic pressure (Achilli et al., 2009; Cornelissen et al., 2008). However, similar to other membrane separation processes, membrane fouling is one of the major challenges to the operation of the OMBR system. Membrane fouling not only reduces water production, enlarges operating and capital costs but also deteriorates membrane lifespan (Luo et al., 2018a). Regular membrane cleaning is therefore required to mitigate the membrane fouling issue during the operation of the OMBR system. Membrane cleaning and fouling mitigation strategies are dependent upon the configuration of membrane and its module. As for submerged membrane modules, membrane cleaning needs to be carried out outside the bioreactor while side stream modules can be physically and chemically cleaned in place. Thus, the membrane and module configurations play a crucial role in mitigating the membrane fouling issues in OMBR.

Lacking a desired FO membrane has remained a hurdle for the FO process and the OMBR system to demonstration and commercialization (Yap et al., 2012). An ideal FO membrane not only can facilitate the execution of membrane fouling mitigation strategies but also can alleviate intrinsic shortcomings of the OMBR system such as high salinity accumulation, critical water flux decline. This ideal membrane should have the following properties: [i] high water permeability, [ii] high solute rejection, and [iii] high membrane-fouling resistance (Tran et al., 2019). The ideal membrane should also possess reasonably mechanical property to prevent breakage and damage during its operation in harsh conditions. Albeit many research studies have recently been conducted to investigate the performance of different membrane and membrane module configurations in OMBR processes, most of these studies used cellulose triacetate (CTA) membrane and/or thin film composite (TFC) polyamide membrane under the flat-sheet configuration (Aftab et al., 2017; Morrow et al., 2018a; Pathak et al., 2018).

There has been only one OMBR study conducted using FO membrane under the configuration of hollow fiber which was made by Zhang et al. (2012). That study used a home-made hollow fiber membrane called inner-selective hollow fiber (ISHF) membrane having a polyamide selective layer coated on the inner side of the fiber. Since the selective layer is in the bore side of the fiber, the application of the ISHF TFC membrane into the OMBR system for wastewater treatment and reuse poses some significant challenges. In their study, Zhang et al. (2012) operated the OMBR system under the orientation of active layer faces draw solution (AL–DS) mode, in which membrane support layer with large-size pores faces the activated sludge containing various types of particulates and foulants. This most likely leads to the deposition and accumulation of particulates and foulants inside the pores, gradually blocking the pore and consequently undermining overall OMBR's performance. Once foulants and particulates enter inside the pores of support layer, membrane fouling becomes a severe issue and fouling mitigation will be a great challenge. On the other hand, when active layer faces feed solution (AL-FS) orientation, activated sludge is circulated into lumen side of ISHF TFC membrane where active layer is coated. Due to the small inner diameter of hollow fiber and the presence of foulants, and flocculated sludge in activated sludge, supplying feed solution into bore side of ISHF membrane can be a considerable challenge. Clogging and blockage might easily occur at the lumen side of ISHF membrane, leading to breakage and damage of membrane or deterioration of membrane's performance (Tran et al., 2019). Fouling control in this case will be a challenging task. Therefore, a hollow fiber membrane having active layer coated on the outer surface is preferred for OMBR application. In comparison with ISHF TFC membrane, an outer selective hollow fiber (OSHF) TFC membrane offers several advantages including larger unit membrane surface area, less membrane fouling potential, and more straightforward membrane fouling control (Le et al., 2016). Recently, a polyethersulfone (PES)-based OSHF TFC FO membrane, having polyamide layer coated on the outer surface of hollow fiber, was successfully developed in our laboratory (Lim et al., 2019). This newly fabricated hollow fiber membrane exhibited comparatively high performance and low fouling propensity, which is considered suitable membrane for the OMBR system treating municipal wastewater for reclamation.

This study aimed to assess the effect of different cross flow velocities (CFVs) and air scouring on membrane fouling mitigation and the performance of our home-made OSHF TFC FO membrane under side-stream configuration in the OMBR system OMBR system. Three different CFVs were applied to recirculate mixed liquor serving as feed solution into the side-stream module of OSHF TFC FO membranes. The performance of the OMBR system in terms of water flux, salinity buildup in the mixed liquor, contaminants removal efficiency, and membrane fouling mitigation, was assessed under AL–FS orientation. We also evaluated the fouling mitigation efficiency of air scouring as a fouling control strategy by regularly injecting air bubble into the membrane module. Findings from this study provide important implications to optimize the operating condition of the OMBR system using the side-stream module of OSHF TFC FO membrane for treating municipal wastewater.

2. Materials and methods

2.1. OSHF TFC FO membrane and module.

This study used a side-stream membrane module containing OSHF TFC FO membrane developed at Center for Technology in Water and Wastewater, University of Technology Sydney, Australia. The properties of this membrane and the side-stream membrane module were mentioned in our previous studies (Lim et al., 2019; Tran et al., 2019).

2.2. Determination of optimum draw solution cross flow velocity

Before the optimization of CFV for FS stream in the OMBR system, side-stream membrane module was firstly used for determination of optimum CFVs for DS stream. A lab-scale FO experiment setup was employed for the optimization of CFVs at DS stream. Optimization of DS's CFV was based on the performance (water flux and reverse salt

Table 1
Experimental conditions for optimization of DS's CFV at a temperature of 22 ± 1 °C, using deionized (DI) water as FS.

No.	Feed solution (2 L)	Draw solution (2 L)	Flowrate (ml/min)		CFV (cm/s)		Orientation	Experiment time (minutes)
			DS	FS	DS	FS		
1	DI water	35 g/L	9	600	5.1	5.1	AL – FS	60
2	DI water	35 g/L	9	1000	5.1	8.5	AL – FS	60
3	DI water	35 g/L	9	1400	5.1	11.9	AL – FS	60
4	DI water	35 g/L	15	600	8.5	5.1	AL – FS	60
5	DI water	35 g/L	15	1000	8.5	8.5	AL – FS	60
6	DI water	35 g/L	15	1400	8.5	11.9	AL – FS	60
7	DI water	35 g/L	21	600	11.9	5.1	AL – FS	60
8	DI water	35 g/L	21	1000	11.9	8.5	AL – FS	60
9	DI water	35 g/L	21	1400	11.9	11.9	AL – FS	60
10	DI water	35 g/L	25	1000	13.9	8.5	AL – FS	60
11	DI water	35 g/L	30	1000	16.7	8.5	AL – FS	60
12	DI water	35 g/L	36	1000	20.1	8.5	AL – FS	60

flux) of FO experiments using our home-made OSHF TFC FO membrane module. These experiments were conducted with conditions as tabulated in Table 1.

2.3. Side-stream OMBR system

Fig. 1 illustrates the schematic diagram of a bench-scale OMBR system used in this study.

2.4. Wastewater influent and draw solution

This study used chemicals with the reagent grade supplied by Merck (Australia). The OMBR system was fed daily with synthetic wastewater comprising of 50 mg/L yeast, 10 mg/L $FeSO_4$, 300 mg/L glucose, 30 mg/L urea, 15 mg/L KH_2PO_4, and 60 mg/L $(NH_4)_2SO_4$. This synthetic influent contained 104.7 ± 10.0 mg/L total organic carbon (TOC), 16.5 ± 1.3 mg/L ammonium nitrogen (NH_4^+), 26.3 ± 0.7 mg/L total nitrogen (TN), and 3.4 ± 0.1 mg/L phosphate (PO_4^{3-}). DS was sodium chloride (NaCl) solution having a concentration of 35 g/L.

2.5. OMBR system operation

Activated sludge used in this study was taken from the recycled water facility at Central Park, Sydney, Australia. The acclimatization of sludge was carried out for more than six months until the system achieved relatively consistent TOC removal efficiency of more than 90%. The concentration of the acclimatized activated sludge was subsequently adjusted to 8.0 g/L before being employed for operation of the OMBR system. A floating valve was used to maintain the continuous feeding of the synthetic wastewater effluent into the OMBR system. To maintain the dissolved oxygen concentration in the bioreactor at a level of more than 3 mg/L for microorganisms, aeration with an intensity of 3 L/min was supplied by an air diffuser (Aqua One, Australia). Activated sludge was recirculated as FS inside the membrane module. Mixed liquor's pH and salinity were regularly monitored by a HQ40D portable pH and conductivity meter (HACH, Germany). DS was recirculated in the bore side of OSHF membrane module from the DS tank. The DS concentration in our experiments was maintained stable at 35 ± 1 g/L by monitoring TDS of DS and using a programmable timer switch connecting with a peristaltic pump (Masterflex, Cole-Parmer, USA) to regularly supplement highly concentrated (5 M) NaCl solution to DS tank. All experiments were conducted in a laboratory with a
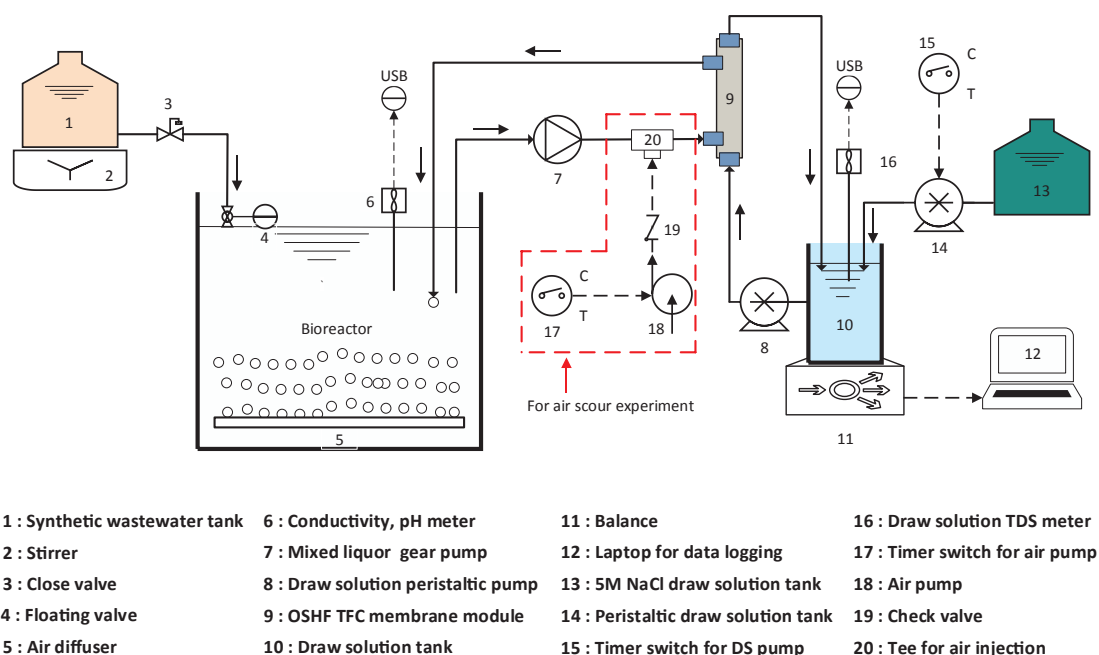

1 : Synthetic wastewater tank 6 : Conductivity, pH meter 11 : Balance 16 : Draw solution TDS meter
2 : Stirrer 7 : Mixed liquor gear pump 12 : Laptop for data logging 17 : Timer switch for air pump
3 : Close valve 8 : Draw solution peristaltic pump 13 : 5M NaCl draw solution tank 18 : Air pump
4 : Floating valve 9 : OSHF TFC membrane module 14 : Peristaltic draw solution tank 19 : Check valve
5 : Air diffuser 10 : Draw solution tank 15 : Timer switch for DS pump 20 : Tee for air injection

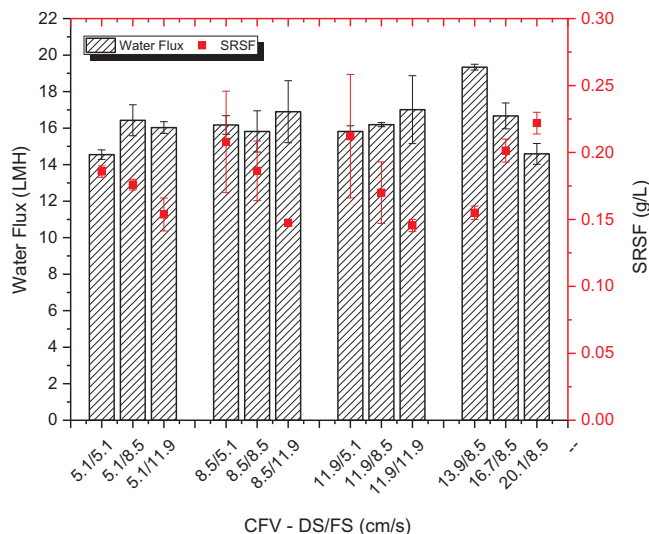**Fig. 1.** Schematic diagram of side-stream osmotic membrane bioreactor system.

Fig. 2. Effects of different DS's cross-flow velocities on FO performance (J_w and specific reverse solute flux - SRSF). Experiment conditions: DS = 35 g/L NaCl; FS = DI water; Temperature = 22 ± 1 °C; AL – FS orientation.

highly controlled environment with an ambient temperature of 22 ± 1 °C. The DS tank and the bioreactor were operated under ambient conditions and the mixed liquor from the same bioreactor was fed to the side-stream FO module.

2.6. Using air scouring as a fouling mitigation strategy

Air bubble with an intensity of 2 L/min was regularly injected into membrane module in order to mitigate the severity of membrane fouling issue on the performance of the OMBR system using side-stream OSHF TFC membrane module. This air injection system consists of an air pump controlled by a programmable timer switch, a check valve preventing diversion of mixed liquor into the air pump when it is not in operation. Before being injected into the membrane module, air bubble and activated sludge were mixed using a connecting tee. This air injection operated under a programmed basis of every two hour, running for 5 min.

2.7. Analytical methods

2.7.1. Water flux, reverse solute flux and specific reverse solute flux determination

Water flux – J_w (L/m² h – LMH) was calculated by Eq. (1):

$$J_w = \frac{\Delta V}{A_m \times \Delta t} \qquad (1)$$

where: A_m (m²) is an effective area of FO membrane; Δt (h) is time interval; ΔV is the net volume change of DS solution (L)

When DI water is used as FS, reverse solute flux – J_s (g/m² h – gMH) was calculated using Eq. (2):

$$J_s = \frac{\Delta V \times \Delta C_t}{A_m \times \Delta t} \qquad (2)$$

where: ΔV and ΔC_t are the net changes in the FS volume (L) and FS's salt concentration; Δt (h) and A_m (m²) are same as in Eq. (1).

Subsequently, specific reverse solute flux (SRSF) was determined by Eq. (3):

$$SRSF = \frac{J_s}{J_w} \qquad (3)$$

2.7.2. Measurement of water quality parameters

The analysis of chemical oxygen demand (COD), mixed liquor suspended solids (MLSS), and mixed liquor volatile suspended solids (MLVSS) was conducted using standard methods for the examination of water and wastewater (APHA, 2005). Dissolved oxygen concentration in the activated sludge during experiments was monitored using a DO meter (Vernier, USA). Water samples of wastewater influent, supernatant and diluted draw solution were regularly collected for measurement of some main contaminants and nutrients for contaminant removal analysis. TOC concentration measurement was conducted using a TOC analyzer Analytikjena Multi N/C 2000. NH_4^+, total nitrogen (TN) and PO_4^{3-} concentrations were measured using corresponding test kits and photometer (Spectroquant, NOVA 60, Merck). Water samples were pretreated and diluted several times if necessary to ensure the correct range of analytes and minimize the interference of chloride.

2.7.3. Membrane characterization

Virgin membrane and fouled membrane samples were collected at the end of each experiment for morphological structures and elemental composition analysis. Samples were dried at room temperature before being coated with gold in a high vacuum sputter coater (EM ACE600, Leica). Subsequently, membrane samples were analyzed in a field emission scanning microscope and energy diffusive X-ray (EDX) analyzer (FE-SEM, Zeiss Supra 55VP, Carl Zeiss AG).

3. Results and discussion

3.1. Optimum cross flow velocity of draw stream.

Fig. 2 illustrates water fluxes and SRSF of OSHF TFC FO membrane during the optimization of CFV on DS and FS streams using DI water. Generally, water fluxes slightly increased with the increase of DS's CFVs from 5.1 cm/s to 11.9 cm/s while SRSF faintly declined when FS's CFVs increased from 5.1 cm/s to 11.9 cm/s. The insignificant drop of SRSF could be attributed to the combined effect of the increase in J_w and a decrease in RSF when FS's CFV accelerated. The increase of FS's CFV might induce low hydraulic pressure on the feed side and consequently resulted in the marginal increase in J_w and the slight drop in RSF (Blandin et al., 2018). Among three CFVs applied on the FS stream, only at CFV of 5.1 cm/s, J_w and SRSF escalated with the increase in DS's CFV. This might be due to the pressure buildup inside the hollow fiber generated a marginal hydraulic pressure, enhancing the mass transport from draw to feed stream by the pressure and hence higher SRSF.

Since the insignificant variations of water fluxes and SRSF were observed during the CFV optimization of both DS and FS streams. DS's CFV was further investigated by increasing CFV to 13.9 cm/s; 16.7 cm/s; and 20.1 cm/s while maintaining FS's CFV at 8.5 cm/s. The results of further investigation are presented in Fig. 2, suggesting that using a CFV of 13.9 cm/s produced the highest J_w of 19.34 LMH and the lowest SRSF of 0.16 g/L. The J_w increase could be attributed to the less severity of dilutive external concentration polarization (DECP) because high CFV generated by high flowrate of DS rapidly replaced the diluted DS stream in the bore side of hollow fiber by a new high concentrated DS, hence reduced the effects of DECP. However, further increasing CFV of DS over 13.9 cm/s resulted in the decline in J_w and the increase in SRSF. This might be ascribed to marginally higher transmembrane pressure induced by high CFV in the lumen side of hollow fiber, hindering the transportation of water from the feed solution through membrane and forcing draw solutes reversely diffusing through the membrane to the feed side (Blandin et al., 2018). Among CFVs of both DS and FS streams, the highest J_w and lowest SRSF were achieved using DS's CFV of 13.9 cm/s and FS's CFV of 8.5 cm/s. Therefore, DS's CFV of 13.9 cm/s was chosen for the optimization of FS's CFV in the OMBR system.
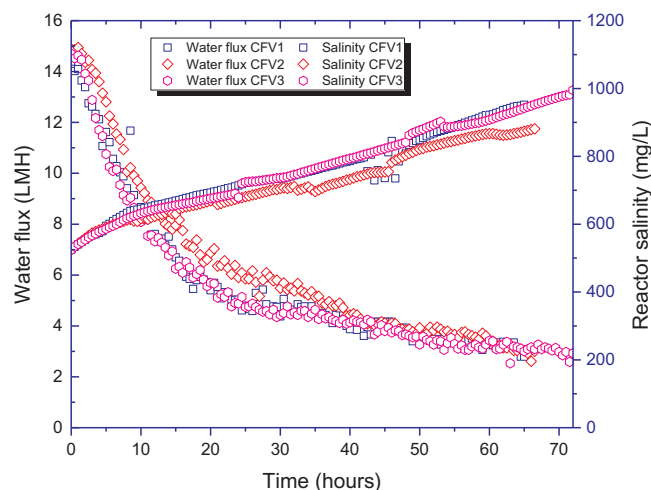
Fig. 3. Water flux profiles and salinity of mixed liquor in the OMBR system under three different cross-flow velocities of feed stream. Experiment conditions: DS = 35 g/L NaCl; FS = activated sludge mixed liquor; Temperature = 22 ± 1 °C; AL – FS orientation. CFV 1 = 5.1 cm/s; CFV 2 = 8.5 cm/s; CFV 3 = 11.9 cm/s.

3.2. Effect of FS's CFV on performance of OSHF TFC FO membrane.

Fig. 3 shows water flux and reactor salinity profiles of the OMBR system using three different CFVs on FS stream. Generally, insignificant differences were observed during the optimization of FS's CFV. The initial water fluxes were 14.4 LMH, 14.9 LMH, and 14.7 LMH when FS's CFV increased from CFV 1 (5.1 cm/s) to CFV 2 (8.5 cm/s), and to CFV 3 (11.9 cm/s), respectively, while DS's CFV was maintained at 13.9 cm/s. Water fluxes of the OMBR system under three different FS's CFVs then continuously declined by 80% after an operation time of 65 h, 67 h, and 72 h, correspondingly. Although there were marginal differences in flux decline magnitude, higher FS's CFV led to a slower reduction in water flux since osmotic net driving forces were relatively similar under three different operating conditions (DS was maintained at the same concentration of 35 g/L and reactor salinities (FS concentration) were moderately similar). Flux decline occurred as a result of combined effect comprising of membrane fouling and decrease in net osmotic driving force due to salinity accumulation in feed solution (mixed liquor) (Luo et al., 2017; Zhang et al., 2017). This result well agrees with an observation by Pathak et al. (2017) that flux drop can also be ascribed to severe membrane fouling, forming a fouling-cake layer on the selective layer. This fouling layer works as an additional barrier hindering water permeation through FO membrane.

Salinity build-up in the mixed liquor is inevitable in the OMBR system treating industrial or municipal wastewater (Wang et al., 2014a). As an inherent property of FO process, salinity accumulation occurred due to the reverse diffusion of draw solute from DS in association with the excellent rejection of FO membrane, retaining salts entering the bioreactor with the influent (Luo et al., 2017; Tran et al., 2019). The elevated activated sludge's TDS concentration not only resulted in a reduction in the net osmotic driving force for water permeation but also potentially inhibited the growth and functionality of microorganism, affecting the biological treatment efficacy (Holloway et al., 2015a). As can be seen from Fig. 3, mixed liquor's TDSs in the OMBR system under three different CFVs gradually increased with a similar pattern. Similar to flux decline, there was an insignificant difference in the increasing intensity of mixed liquor's TDSs. Starting at a TDS of 525 mg/L, salinity in the reactor reached to 952 mg/L after 65-h operation using a CFV1 of 5.1 cm/s, 881 mg/L after 67-hour operation using a CFV2 of 8.5 cm/s, and 995 mg/L after 72-h operation using a CFV3 of 11.9 cm/s. The slightly faster increase of mixed liquor's TDS using CFV1 compared to that using CFV2 might be ascribed to the

enhanced solute transport from DS induced by slightly higher hydraulic pressure inside the hollow fiber when much higher CFV (13.9 cm/s) was applied on DS side than that on FS one (5.1 cm/s).

Membrane fouling in FO processes and OMBR is commonly known as reversible due to the absence of hydraulic pressure (Lutchmiah et al., 2014). Therefore, simple physical cleaning method such as increasing CFV of the feed solution can alleviate the severity of FO membrane fouling issues. Increasing CFV not only helps to mitigate membrane fouling but also reduces the effect of DECP. Foulant accumulation was found to be less under higher CFV, thereby leading to the formation of a much thinner and looser fouling-cake layer. Elevated CFV also generates greater turbulence and hydraulic shear forces to remove the loose and sparse FO fouling-cake layer (Li et al., 2012). Several previously reported research studies had also proved that flux decline rate became more moderate when higher CFV was applied on FO process (Boo et al., 2013, 2012; Li et al., 2012; Liu and Mi, 2012; Mi and Elimelech, 2010). Nonetheless, the experimental results in this current study showed that no significant impacts of FS's CFV were observed on flux decline rate and salinity accumulation, meaning that membrane fouling in the OMBR system using a side-stream membrane module was not significantly affected by enhanced CFV on feed side. It is hard to fairly compare the effect of FS's CFV on membrane fouling mitigation between this work and previously conducted ones since FS used in these studies were different compared to activated sludge in the OMBR system. For instance, Mi and Elimelech (2010) used FS containing 50 mM NaCl, 200 mg/L alginate, and 0.5 mM CaCl$_2$ while Boo et al. (2012) employed a feed solution comprising of 50 mM NaCl and 1 g/L colloidal particle foulant having size of 139 nm. Li et al. (2012) used pre-filtered natural seawater from the Red sea, being added with 0.02% NaN$_3$ to prevent the growth of bacteria and algae. Using different feed solutions results in a substantial difference in membrane fouling behaviors (Holloway et al., 2015a). Compared to typical FO process not using activated sludge as FS, membrane fouling in OMBR is considered more complicated due to the nature of activated sludge, containing a variety of microorganism and foulants (Ibrar et al., 2019; Zhang et al., 2012). The majority of fouling layer in OMBR was found comprising of a thin gel-like layer determined to be soluble microbial products (SMP) and extracellular polymeric substances (EPS) which are two key foulants in the MBR based system.

3.3. Effect of periodic air scouring on membrane fouling mitigation

Air scouring has been previously reported as an effective membrane fouling mitigation method for OMBR systems. Compared to a system operated at low membrane aeration rate, enhanced membrane air scouring rate reduced 31-fold biomass volume and 12-fold biomass coverage on the membrane surface (Zhang et al., 2014). Holloway et al. (2015b) also reported that vigorous aeration using coarse air bubbles for membrane air scouring improved OMBR's performance by sustaining water flux over 125 days of operation. The result from a FO fouling study conducted by Mi and Elimelech (2008) exhibited a 98% water flux recovery when periodic aeration was introduced to the selective layer of FO membrane facing a synthetic feed solution containing alginate. Therefore, air scouring was used in our study as a fouling mitigation method during OMBR operation. Air bubbles were injected into the side-stream membrane module with a regular basis of 5 min in every two hour.

Fig. 4 shows water flux and reactor salinity profiles of the OMBR system using side-stream module of OSHF TFC FO membrane operated with regular air scouring. Generally, OMBR performance was substantially improved when periodic air bubbles were injected into side-stream membrane module compared to that without air scouring. Water flux of the OMBR system was maintained at above 10.19 LMH which was almost twice higher compared to that of CFV1 without aeration (5.66 LMH) during the first 24 h. The water flux decline rate was much slower and water flux dropped by 80% after a 6-day operation (2-fold
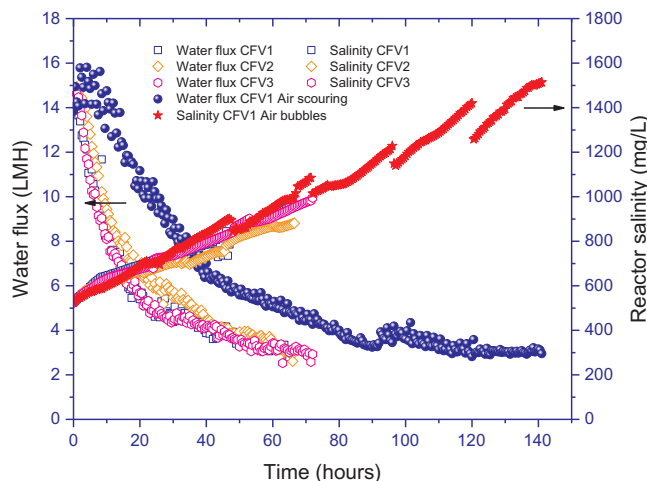
Fig. 4. Water flux profiles and salinity of mixed liquor in the OMBR system under the CFV 1 of feed stream with regular air scouring. Experiment conditions: DS = 35 g/L NaCl; FS = activated sludge mixed liquor; Temperature = 22 ± 1 °C; AL – FS orientation.

longer operation time than OMBR operation without air scouring). However, air scouring showed negligible influence on the accumulation rate of bioreactor salinity, which still followed a similar upward trend compared to that without air bubbles. This result proved that air scouring on the outer surface of hollow fiber effectively mitigated membrane fouling, hence, improved the performance of the OMBR system. The enhancement of water flux in this study is in good agreement with prior research works on conventional MBR using microfiltration/ultrafiltration membrane (Fouladitajar et al., 2014; Javadi et al., 2014) and in OMBR studies (Holloway et al., 2015b; Mi and Elimelech, 2008).

The observed flux improvement can be explained following a mechanism of slug flow in the tubular module (In this study, the air was sparged into a tubular side-stream membrane module of OSHF TFC FO membrane). The injected air bubbles firstly formed slug flows inside the tubular membrane module and subsequently induced secondary flows and wakes. The nascent wakes and secondary flows promote local vortexes near the surface of each hollow fibre membrane (Fouladitajar et al., 2014) which hinders accumulation of foulants on membrane surface. In addition, the air bubbles also create a mixed gas–liquid flow that accelerates the cross flow velocity and enhances wall shear force thereby helping partly remove the accumulated fouling layer on membrane surface (Javadi et al., 2014). Since the formation of the biofilm layer on the membrane surface is impeded, the severity of cake enhanced concentration polarization, potentially caused by biofilm layer, is also disrupted (Zhang et al., 2012). The resistance created by membrane fouling is therefore mitigated thereby improving the water flux. The injection of air bubbles into the membrane module might cause breakage of the hollow fiber membrane and abrasion on the membrane's active layer due to hydrodynamic turbulence generated by air bubbles. While breakage of hollow fiber would be easy to be observed during the operation, damages of the active layer can be detected by the abnormal increase in reverse solute flux which is directly related to salinity build-up in the reactor. However, no breakage or abrasion was observed during the 6-day operation of the OMBR system with air scouring. Overall, it can be concluded that periodic aeration into side-stream module of OSHF TFC FO membrane by air bubbles significantly improved the OMBR performance.

3.4. Removal of pollutants

Removal efficacy of primary pollutants including total organic contaminants (TOC), ammonium NH_4^+, total nitrogen (TN), and

phosphate (PO_4^{3-}) by the OMBR system under three different CFVs and air scouring was also assessed. Samples were collected from wastewater influent, supernatant, and DS tank during each experiment operation time for pollutant and nutrient concentration analysis. This aims to investigate the influence of different operating conditions on pollutant and nutrient removal efficiencies of the OMBR system which is illustrated in Fig. 5. Overall, the OMBR system exhibited consistently high removal efficiencies of TOC, NH_4^+, TN, and PO_4^{3-} and there was an insignificant difference in removal efficiencies between different operating conditions. Biodegradation and high rejection of the OSHF TFC FO membrane were ascribed to effective removal of organic matters and nutrients in an OMBR system (Luo et al., 2018b).

Under three different CFVs and with air scouring operating conditions, the OMBR system achieved a stable TOC removal efficacy of over 98% during experiment time (Fig. 5 (1)). Some prior studies also reported high overall TOC removal in the OMBR system from 98 to 100% by Zhu et al. (2018), 96% by Wang et al. (2016). In another OMBR research work, Achilli et al. (2009) achieved an overall TOC removal of 99% in which FO membrane contributed to 98% rejection. Qiu and Ting (2013) noted that a stable overall TOC removal of up to 98% in their study. Similar to TOC removal, NH_4^+ removals of the OMBR system operated with three CFV values and air scouring were stable at over 98% (Fig. 5 (2)) which were much higher compared to that of 80–90% in a study conducted by Qiu and Ting (2014a). The high removal of NH_4^+ in the OMBR system obtained in this study well agrees with our recent study (Tran et al., 2019) and previous OMBR studies (Achilli et al., 2009; Pathak et al., 2018; Qiu and Ting, 2013; Wang et al., 2014b). The consistently high removal of NH_4^+ was attributed to the biological nitrification and high rejection of the FO membrane (Tran et al., 2019).

Fig. 5 (3) shows the TN removal efficiency of the OMBR system operated under different CFVs and with air scouring. Experimental results from this study exhibited that no significant difference of TN removal efficacy between four operating conditions and that only about 80% TN was removed by the OMBR system. The slight increase of TN concentration in mixed liquor could be attributed to the high rejection of the OSHF TFC FO membrane to nitrogen species including nitrate which is a product of nitrification process of NH_4^+. Since resultant nitrate cannot be converted into nitrogen gas due to lack of denitrification process, TN removal depended upon the biological degradation of microorganism and it was ineffective under aerobic condition (Jin et al., 2019). Luo et al. (2018b) also reported the same result in their OMBR study using aquaporin TFC flat-sheet FO membrane.

Phosphorous removal efficiencies of the OMBR system are illustrated in Fig. 5 (4). Relatively stable and high phosphorous removals were exhibited by the OMBR system under four operating conditions with an overall of approximately 97%. The high and consistent removal of phosphorous was ascribed to microbial assimilation by phosphate accumulating organisms (PAOs) and high rejection of the FO membrane. Shi et al. (2012) reported that biodegradation of phosphorous was inhibited by elevated salinity in activated sludge, affecting the metabolism and activities of PAOs. Phosphate removal, therefore, mainly depends on the rejection of a FO membrane to PO_4^{3-}. Having relatively large radius diameter (0.49 nm) and negative charge, orthophosphate ions were almost completely rejected by the FO membrane (Pathak et al., 2017). Excellent phosphorous removal of the OMBR system was also reported by Nguyen et al. (2016) with efficiency of 98%.

It can be concluded that FS's CFV without and with air scouring showed a minor difference on the performance of the OMBR system in terms of pollutant removals, with consistent and high removal efficacies of targeted pollutants. These results also proved the durability of our home-made OSHF TFC FO membrane, being able to withstand various harsh operating conditions as tested.
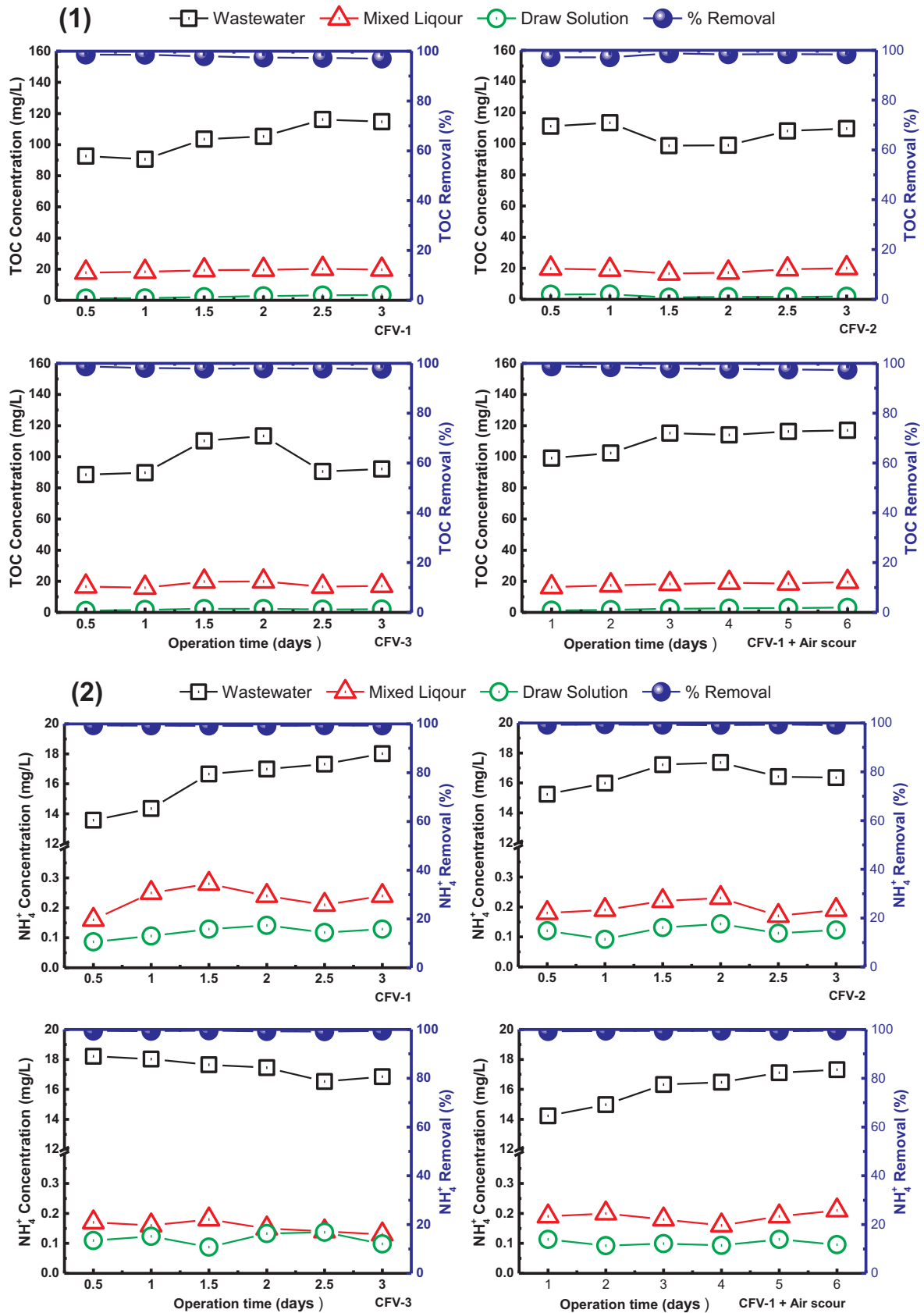
Fig. 5. Removal of pollutants of OMBR system operated under different cross flow velocities and with air scouring (1) TOC removal; (2) NH$_4^+$ removal; (3) TN removal; and (4) PO$_4^{3-}$.
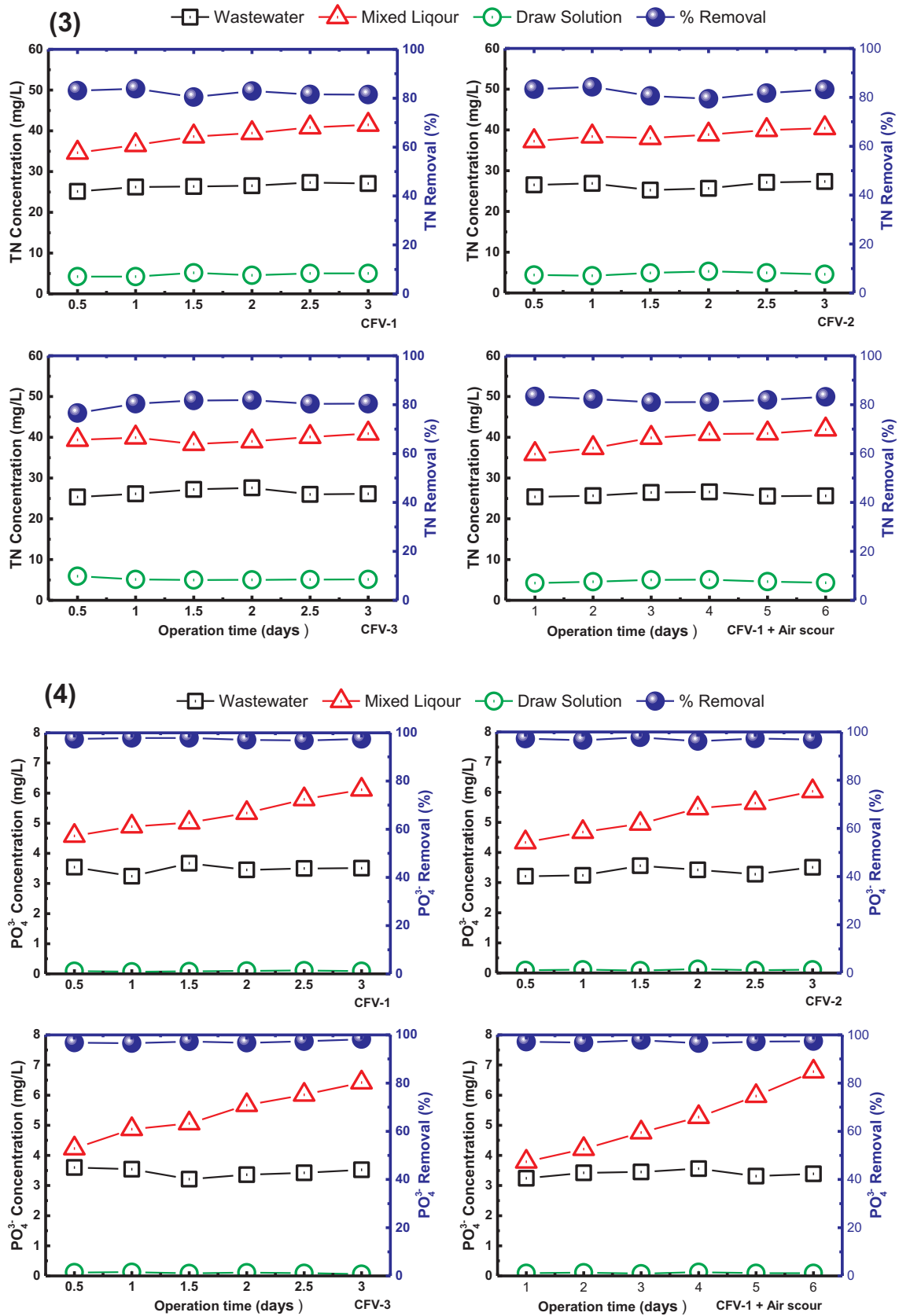
Fig. 5. (*continued*)

Table 2
The elemental compositions of virgin and fouled membranes by energy-dispersive X-ray (EDX) analysis.

Weight %	C	O	Na	Cl	Ca	Mg	K	Al	Fe
Pristine	61.92	38.08							
CFV 1	53.65	35.00	1.33	2.06	1.43	1.03	3.26	1.05	1.19
CFV 2	57.22	29.11	2.07	3.23	3.90	0.76	2.08	0.56	1.07
CFV 3	48.58	34.26	1.92	4.44	3.90	0.92	3.11	1.69	1.18
CFV 1 + Air scouring	61.42	28.20	1.52	4.76	1.19	0.38	1.54	0.39	0.60

3.5. Membrane and fouling cake layer characterization

Pristine and fouled membrane after each OMBR operation with three different CFVs and air scouring were collected for an autopsy to investigate surface morphologies. A typical ridge-and-valley surface morphology of polyamide selective layer was presented in the surface SEM image of the virgin FO membrane and cross-sectional image also confirms that neither deposition of foulants nor formation of fouling cake layer was found on the outer surface of OSHF TFC FO membrane. SEM images of fouled membranes showed the formation of fouling cake layer with accumulation of different foulants on the outer surface of FO membrane. Interestingly, there was a slight difference in thickness of fouling cake layers under three CFVs investigated. Slow CFV (CFV 1) led to thinner cake layer (45 µm) than those of fast CFVs including CFV 2 and CFV 3 with thickness of 59 µm and 57 µm, respectively. This result indicated that increasing CFV of the FS stream resulted in thicker fouling cake layer, which is contradictory to common expectation that faster CFV generates more powerful shear force to remove the deposition and accumulation of foulants on selective layer. This result is not in good agreement with the one reported by Morrow et al. (2018b). In that study, thinner cake layer in side-stream flat-sheet FO membrane compared to submerged plate and frame membrane module was observed, which was attributed to the compaction of cake layer due to hydraulic pressure in the side-stream membrane module and combined with greater hydraulic scour generated by high CFV. However, it is hard to compare two results, since the configurations of two side-stream membrane modules were different. In our study, a tubular side-stream module was used while the one used by Morrow et al. (2018b) was the one for flat-sheet membrane. Different configuration and water channel spacing might give rise to different distribution of activated sludge flows inside the membrane module, hence difference in membrane fouling behavior. SEM images of fouled FO membrane under OMBR operation with periodic air scouring clearly showed the high effectiveness of using air bubbles for mitigating membrane fouling in the side-stream membrane module. Surface morphology of fouling cake layer was smoother compared to those without air scouring and much thinner cake layer (25 µm) was illustrated in the cross-sectional image.

Table 2 tabulates some selected elements detected in fouling cake layers of fouled FO membrane after OMBR operation with three CFVs and air scouring by EDX analysis. Result of analysis on virgin FO membrane showed two main elements including C and O while fouling-cake layers of the four fouled membranes contain various elements such as Na, Cl, Ca, Mg, K, Al and Fe which are typical ones found in the activated sludge (Pathak et al., 2017). In general, elemental compositions of fouling cake layers were comparatively similar among four collected fouled FO membrane. The existence of Na and Cl could be related to reverse diffusion of draw solute. The source of other inorganic elements was most likely the synthetic wastewater (e.g. Fe, P).

4. Conclusions

Effects of CFV and air scouring on the performance and membrane fouling mitigation of the OMBR system using a side-stream module of OSHF TFC FO membrane were investigated. Generally, performance of the OMBR system in terms of water flux; mixed liquor's salinity accumulation, removal efficiencies of TOC, NH_4^+, TN, and PO_4^{3-} was consistently high and insignificantly influenced by different CFVs and air scouring. However, air scouring effectively mitigated membrane fouling in the side-stream module of OSHF TFC membrane. Findings also indicated that tested periodic air scouring was an efficient method for fouling mitigation without interrupting the normal operation and the performance of the OMBR system.

Declaration of Competing Interest

The authors declare that they have no known competing financial interests or personal relationships that could have appeared to influence the work reported in this paper.

Acknowledgments

Appendix A. Supplementary data

Supplementary data to this article can be found online at https://doi.org/10.1016/j.biortech.2019.122303.

References

Achilli, A., Cath, T.Y., Marchand, E.A., Childress, A.E., 2009. The forward osmosis membrane bioreactor: a low fouling alternative to MBR processes. Desalination 239 (1), 10–21.
Aftab, B., Khan, S.J., Maqbool, T., Hankins, N.P., 2017. Heavy metals removal by osmotic membrane bioreactor (OMBR) and their effect on sludge properties. Desalination 403, 117–127.
APHA, A., WEF, 2005. Standard methods for the examination of water and wastewater. American Public Health Association (APHA): Washington, DC, USA.
Blandin, G., Rodriguez-Roda, I., Comas, J., 2018. Submerged osmotic processes: design and operation to mitigate mass transfer limitations. Membranes 8 (3), 72.
Boo, C., Elimelech, M., Hong, S., 2013. Fouling control in a forward osmosis process integrating seawater desalination and wastewater reclamation. J. Membr. Sci. 444, 148–156.
Boo, C., Lee, S., Elimelech, M., Meng, Z., Hong, S., 2012. Colloidal fouling in forward osmosis: Role of reverse salt diffusion. J. Membr. Sci. 390–391, 277–284.
Chang, H.-M., Sun, Y.-C., Chien, I.C., Chang, W.-S., Ray, S.S., Cao, D.T.N., Cong Duong, C., Chen, S.-S., 2019. Innovative upflow anaerobic sludge osmotic membrane bioreactor for wastewater treatment. Bioresour. Technol. 287 121466.
Cornelissen, E.R., Harmsen, D., de Korte, K.F., Ruiken, C.J., Qin, J.-J., Oo, H., Wessels, L.P., 2008. Membrane fouling and process performance of forward osmosis membranes on activated sludge. J. Membr. Sci. 319 (1), 158–168.
Fouladitajar, A., Zokaee Ashtiani, F., Rezaei, H., Haghmoradi, A., Kargari, A., 2014. Gas sparging to enhance permeate flux and reduce fouling resistances in cross flow microfiltration. J. Ind. Eng. Chem. 20 (2), 624–632.
Holloway, R.W., Achilli, A., Cath, T.Y., 2015a. The osmotic membrane bioreactor: a critical review. Environ. Sci. Water Res. Technol. 1 (5), 581–605.
Holloway, R.W., Wait, A.S., Fernandes da Silva, A., Herron, J., Schutter, M.D., Lampi, K., Cath, T.Y., 2015b. Long-term pilot scale investigation of novel hybrid ultrafiltration-osmotic membrane bioreactors. Desalination 363, 64–74.
Ibrar, I., Naji, O., Sharif, A., Malekizadeh, A., Alhawari, A., Alanezi, A.A., Altaee, A., 2019. A review of fouling mechanisms, control strategies and real-time fouling monitoring techniques in forward osmosis. Water 11 (4).
Javadi, N., Zokaee Ashtiani, F., Fouladitajar, A., Moosavi Zenooz, A., 2014. Experimental studies and statistical analysis of membrane fouling behavior and performance in microfiltration of microalgae by a gas sparging assisted process. Bioresour. Technol. 162, 350–357.
Jin, P., Chen, Y., Xu, T., Cui, Z., Zheng, Z., 2019. Efficient nitrogen removal by simultaneous heterotrophic nitrifying-aerobic denitrifying bacterium in a purification tank bioreactor amended with two-stage dissolved oxygen control. Bioresour. Technol. 281, 392–400.
Kim, Y., Li, S., Chekli, L., Woo, Y.C., Wei, C.-H., Phuntsho, S., Ghaffour, N., Leikness, T., Shon, H.K., 2017. Assessing the removal of organic micro-pollutants from anaerobic membrane bioreactor effluent by fertilizer-drawn forward osmosis. J. Membr. Sci. 533, 84–95.
Le, N.L., Bettahalli, N.M.S., Nunes, S.P., Chung, T.-S., 2016. Outer-selective thin film composite (TFC) hollow fiber membranes for osmotic power generation. J. Membr.

Sci. 505, 157–166.

Li, Z.-Y., Yangali-Quintanilla, V., Valladares-Linares, R., Li, Q., Zhan, T., Amy, G., 2012. Flux patterns and membrane fouling propensity during desalination of seawater by forward osmosis. Water Res. 46 (1), 195–204.

Lim, S., Tran, V.H., Akther, N., Phuntsho, S., Shon, H.K., 2019. Defect-free outer-selective hollow fiber thin-film composite membranes for forward osmosis applications. J. Membr. Sci. 586, 281–291.

Liu, Y., Mi, B., 2012. Combined fouling of forward osmosis membranes: Synergistic foulant interaction and direct observation of fouling layer formation. J. Membr. Sci. 407–408, 136–144.

Luo, W., Arhatari, B., Gray, S.R., Xie, M., 2018a. Seeing is believing: Insights from synchrotron infrared mapping for membrane fouling in osmotic membrane bioreactors. Water Res. 137, 355–361.

Luo, W., Phan, H.V., Xie, M., Hai, F.I., Price, W.E., Elimelech, M., Nghiem, L.D., 2017. Osmotic versus conventional membrane bioreactors integrated with reverse osmosis for water reuse: biological stability, membrane fouling, and contaminant removal. Water Res. 109, 122–134.

Luo, W., Xie, M., Song, X., Guo, W., Ngo, H.H., Zhou, J.L., Nghiem, L.D., 2018b. Biomimetic aquaporin membranes for osmotic membrane bioreactors: membrane performance and contaminant removal. Bioresour. Technol. 249, 62–68.

Lutchmiah, K., Verliefde, A.R.D., Roest, K., Rietveld, L.C., Cornelissen, E.R., 2014. Forward osmosis for application in wastewater treatment: a review. Water Res. 58, 179–197.

Mi, B., Elimelech, M., 2008. Chemical and physical aspects of organic fouling of forward osmosis membranes. J. Membr. Sci. 320 (1), 292–302.

Mi, B., Elimelech, M., 2010. Organic fouling of forward osmosis membranes: fouling reversibility and cleaning without chemical reagents. J. Membr. Sci. 348 (1), 337–345.

Morrow, C.P., Furtaw, N.M., Murphy, J.R., Achilli, A., Marchand, E.A., Hiibel, S.R., Childress, A.E., 2018a. Integrating an aerobic/anoxic osmotic membrane bioreactor with membrane distillation for potable reuse. Desalination 432, 46–54.

Morrow, C.P., McGaughey, A.L., Hiibel, S.R., Childress, A.E., 2018b. Submerged or sidestream? The influence of module configuration on fouling and salinity in osmotic membrane bioreactors. J. Membr. Sci. 548, 583–592.

Nguyen, N.C., Chen, S.-S., Nguyen, H.T., Ray, S.S., Ngo, H.H., Guo, W., Lin, P.-H., 2016. Innovative sponge-based moving bed–osmotic membrane bioreactor hybrid system using a new class of draw solution for municipal wastewater treatment. Water Res. 91, 305–313.

Pathak, N., Chekli, L., Wang, J., Kim, Y., Phuntsho, S., Li, S., Ghaffour, N., Leikness, T., Shon, H., 2017. Performance of a novel baffled osmotic membrane bioreactor-microfiltration hybrid system under continuous operation for simultaneous nutrient removal and mitigation of brine discharge. Bioresour. Technol. 240, 50–58.

Pathak, N., Li, S., Kim, Y., Chekli, L., Phuntsho, S., Jang, A., Ghaffour, N., Leikness, T.,

Shon, H.K., 2018. Assessing the removal of organic micropollutants by a novel baffled osmotic membrane bioreactor-microfiltration hybrid system. Bioresour. Technol. 262, 98–106.

Qiu, G., Ting, Y.-P., 2014a. Direct phosphorus recovery from municipal wastewater via osmotic membrane bioreactor (OMBR) for wastewater treatment. Bioresour. Technol. 170, 221–229.

Qiu, G., Ting, Y.-P., 2013. Osmotic membrane bioreactor for wastewater treatment and the effect of salt accumulation on system performance and microbial community dynamics. Bioresour. Technol. 150, 287–297.

Qiu, G., Ting, Y.-P., 2014b. Short-term fouling propensity and flux behavior in an osmotic membrane bioreactor for wastewater treatment. Desalination 332 (1), 91–99.

Shi, K., Zhou, W., Zhao, H., Zhang, Y., 2012. Performance of halophilic marine bacteria inocula on nutrient removal from hypersaline wastewater in an intermittently aerated biological filter. Bioresour. Technol. 113, 280–287.

Tran, V.H., Lim, S., Han, D.S., Pathak, N., Akther, N., Phuntsho, S., Park, H., Shon, H.K., 2019. Efficient fouling control using outer-selective hollow fiber thin-film composite membranes for osmotic membrane bioreactor applications. Bioresour. Technol. 282, 9–17.

Wang, X., Chen, Y., Yuan, B., Li, X., Ren, Y., 2014a. Impacts of sludge retention time on sludge characteristics and membrane fouling in a submerged osmotic membrane bioreactor. Bioresour. Technol. 161, 340–347.

Wang, X., Yuan, B., Chen, Y., Li, X., Ren, Y., 2014b. Integration of micro-filtration into osmotic membrane bioreactors to prevent salinity build-up. Bioresour. Technol. 167, 116–123.

Wang, Z., Zheng, J., Tang, J., Wang, X., Wu, Z., 2016. A pilot-scale forward osmosis membrane system for concentrating low-strength municipal wastewater: performance and implications. Sci. Rep. 6, 21653.

Yap, W.J., Zhang, J., Lay, W.C.L., Cao, B., Fane, A.G., Liu, Y., 2012. State of the art of osmotic membrane bioreactors for water reclamation. Bioresour. Technol. 122, 217–222.

Zhang, B., Song, X., Nghiem, L.D., Li, G., Luo, W., 2017. Osmotic membrane bioreactors for wastewater reuse: Performance comparison between cellulose triacetate and polyamide thin film composite membranes. J. Membr. Sci. 539, 383–391.

Zhang, J., Loong, W.L.C., Chou, S., Tang, C., Wang, R., Fane, A.G., 2012. Membrane biofouling and scaling in forward osmosis membrane bioreactor. J. Membr. Sci. 403–404, 8–14.

Zhang, Q., Jie, Y.W., Loong, W.L.C., Zhang, J., Fane, A.G., Kjelleberg, S., Rice, S.A., McDougald, D., 2014. Characterization of biofouling in a lab-scale forward osmosis membrane bioreactor (FOMBR). Water Res. 58, 141–151.

Zhu, W., Wang, X., She, Q., Li, X., Ren, Y., 2018. Osmotic membrane bioreactors assisted with microfiltration membrane for salinity control (MF-OMBR) operating at high sludge concentrations: Performance and implications. Chem. Eng. J. 337, 576–583.